Environmental Toxicology and Pharmacology 96 (2022) 104005

Contents lists available at ScienceDirect

Environmental Toxicology and Pharmacology

journal homepage: www.elsevier.com/locate/etap

Ubiquitin proteasomal system is a potential target of the toxic effects of organophosphorus flame retardant triphenyl phosphate

Ayse Tarbin Jannuzzi [a,*], Ayse Mine Yilmaz Goler [b], Buket Alpertunga [a,c,**]

[a] Department of Pharmaceutical Toxicology, Faculty of Pharmacy, Istanbul University, Istanbul, Turkey
[b] Department of Biochemistry, School of Medicine/Genetic and Metabolic Diseases Research and Investigation Center, Marmara University, Istanbul, Turkey
[c] Department of Pharmaceutical Toxicology, Faculty of Pharmacy, Istanbul Health and Technology University, Istanbul, Turkey

ARTICLE INFO

Edited by Dr. M.D. Coleman

Keywords:
Triphenyl phosphate
Proteasome activity
Oxidative stress
Heat shock stress
Endoplasmic reticulum stress

ABSTRACT

The consumption of the widely used flame retardant Triphenyl phosphate (TPP) is increasing. It is now frequently detected in the environment and also domestically. Although the possibility of dermal exposure to TPP is quite high, little is known about its potential molecular toxicity mechanisms. In this study, we found that TPP caused cytotoxicity on human skin keratinocytes (HaCaT) and significantly inhibited the proliferation and cell migration in a concentration-dependent manner. Additionally, HaCaT cells were sensitive to TPP-induced apoptosis. Reactive oxygen species production was induced with TPP, which increased the protein carbonylation and lipid peroxidation levels. Moreover, TPP inhibited proteasome activity and increased the accumulation of ubiquitinated proteins. Exposure to TPP significantly increased the HSP90, HSP70, GRP94 and GRP78 protein levels. Overall, our findings indicate that TPP may pose a risk to human health and contribute to the current understanding of the risks of TPP at the molecular level.

1. Introduction

Triphenyl phosphate (TPP) is one of the most commonly used organophosphorus flame retardants. It is used as a plasticizer and an additive for the manufacture of many different products such as textiles, plastic, electronics, foams, and nail polishes (Mendelsohn et al., 2016; WHO, 1991). Due to its use as an additive, TPP is not chemically bound to these products and enters the environment mainly by leaching and volatilization(van der Veen and de Boer, 2012). TPP is frequently detected in various consumer products and widely found in environmental samples including indoor house dust, hand wipes (Hoffman et al., 2015; Meeker and Stapleton, 2010; Stapleton et al., 2009), indoor air (Saito et al., 2007), surface water (Andresen et al., 2004; Zhang et al., 2018) and drinking water (Li et al., 2014). A number of studies have been conducted to evaluate the toxicity of TPP and concerns have been raised over the human health risks of TPP (van der Veen and de Boer, 2012). There are different in vitro and in vivo studies indicating the endocrine disrupting properties of TPP (Chen et al., 2015; Kojima et al., 2013; Liu et al., 2012; Wang et al., 2018). Further reports showed that TPP can disturb lipid metabolism and cause lipid accumulation, induce endoplasmic reticulum stress and inflammation in different cell lines (Hu et al., 2020; Wang et al., 2021). Also, TPP causes metabolic dysfunction in animal models (Wang et al., 2019), and TPP-induced developmental and cardiac toxicities have been reported (Qi et al., 2019). TPP can pass the blood-brain barrier and be potentially neurotoxic (Liu et al., 2020). The possible toxic mechanisms of TPP include increased endoplasmic reticulum and oxidative stress, activated inflammatory responses, cell cycle arrest and apoptosis (Chen et al., 2015; Hu et al., 2020; Qi et al., 2019; Wang et al., 2020).

The ubiquitin proteasomal system is the main proteolytic pathway for the degradation of short-lived, damaged and misfolded proteins in the cells. The inhibition of proteasome activity leads to accumulation of misfolded and damaged proteins, and to the failure of amino acid-recycling which leads to proteotoxicity (Jung et al., 2009). Recent studies have demonstrated that TPP can alter ubiquitin proteasomal system-related proteins (Kim et al., 2020; Wang et al., 2020). However, no study has yet focused on the activity of the proteasome. Therefore, it is important to understand the role of the ubiquitin proteasomal system in clarifying the adverse effects of TPP.

Biomonitoring of TPP in exposed groups has shown that one of the main routes for TPP exposure is dermal (Estill et al., 2020; Liu et al., 2017; Mendelsohn et al., 2016) along with hand-to-mouth transfer,

* Correspondence to: Department of Pharmaceutical Toxicology, Faculty of Pharmacy, Istanbul University, 34116 Istanbul, Turkey.
** Corresponding author at: Department of Pharmaceutical Toxicology, Faculty of Pharmacy, Istanbul Health and Technology University, Istanbul, Turkey.
E-mail addresses: tarbin.cevik@istanbul.edu.tr (A.T. Jannuzzi), tunga@istanbul.edu.tr (B. Alpertunga).

https://doi.org/10.1016/j.etap.2022.104005
Received 17 January 2022; Received in revised form 16 August 2022; Accepted 25 October 2022
Available online 7 November 2022

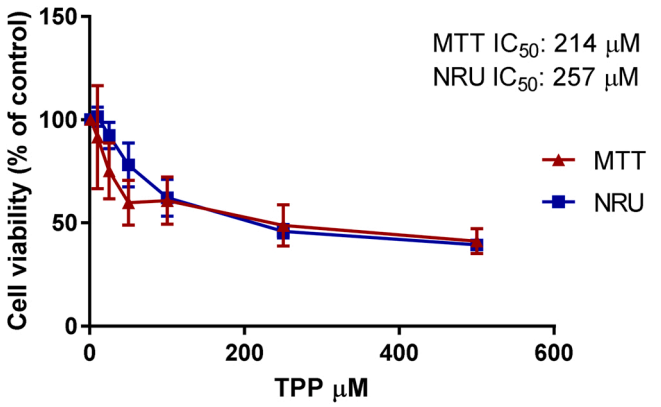

Fig. 1. Dose-dependent effects of TPP on HaCaT cell viability after 24 h treatment by the MTT and NRU assays. Values represent mean ± SD. IC_{50}: Inhibitor concentration 50.

ingestion of TPP contaminated food and water, and inhalation through ambient air (Betts, 2015; Xu et al., 2016). Biomonitoring studies also indicate that after dermal absorption, TPP metabolites can be determined in the urine (Jayatilaka et al., 2019; Mendelsohn et al., 2016). Nevertheless, despite a growing number of studies aiming to clarify the toxic potential of TPP, knowledge regarding its effects on dermal exposure remains scarce. Thus in this study, we aimed to investigate the in vitro molecular effects of TPP on human dermal keratinocytes (HaCaT cells) as an exposure pathway-related cell line.

2. Material and methods

2.1. Chemicals

TPP was bought from Merck. The HaCaT cell line was obtained from ThermoFisher. All of the cell culture materials were purchased from Gibco. The apoptosis/necrosis assay kit was obtained from Invitrogen. 3-[4,5-dimethylthiazol-2-yl]− 2,5-diphenyl-tetrazolium bromide (MTT), neutral red dye, dimethyl sulfoxide (DMSO) were from Biomatik. of 5′, 6′-chloromethyl-2′,7′-dichlorofluorescein diacetate (H_2DCFDA) dye and Bradford reagent were bought from Sigma-Aldrich. HSP90, HSP70, GRP94 and GRP78 antibodies were obtained from Cell Signaling. HRP conjugated anti-rabbit and anti-mouse, ubiquitin, GAPDH, HSP40 antibodies and RIPA buffer were from SCBT. Human Protein Carbonyl ELISA Kit was obtained from BT-Lab. Thiobarbituric acid (TBARS) Assay Kit was bought from RayBiotek. All other chemicals were from Sigma-Aldrich if not otherwise stated.

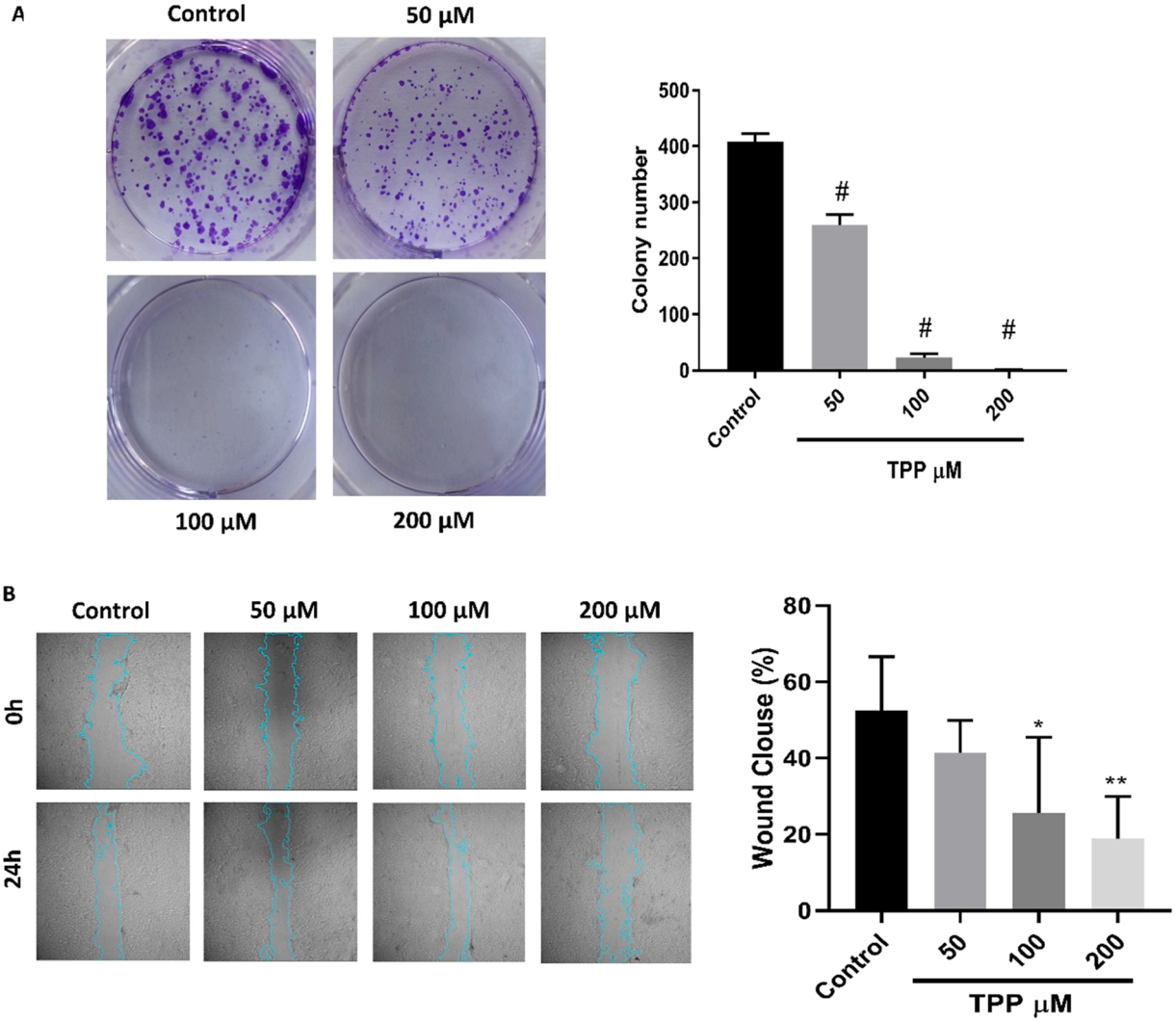

Fig. 2. Dose-dependent effects of TPP on HaCaT cell proliferation (A) and migration capacities (B) after 24 h treatment with the colony formation and scratch assays. Values represent mean ± SD. * $p < 0.05$, * * $p < 0.01$, $^{\#}p < 0.0001$ versus control group.

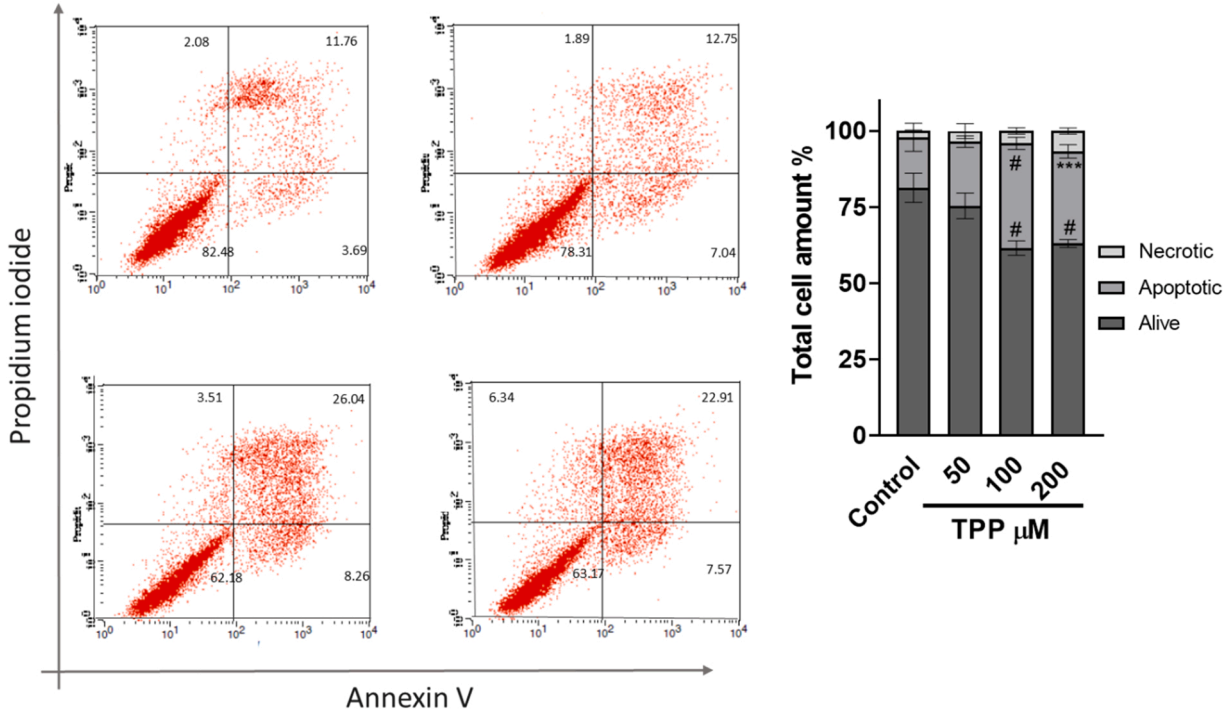

Fig. 3. Apoptosis necrosis induction in HaCaT cells after TPP treatment for 24 h. Representative images of flow cytometry-determined apoptosis by Annexin V/PI staining. Values represent mean ± SD. * ** $p < 0.001$, $^{\#}p < 0.0001$ versus control group.

2.2. Cell culture and treatments

HaCaT human keratinocytes were cultured in Dulbecco's Modified Eagle Medium with high glucose, L-glutamine, HEPES supplemented with 10 % fetal bovine serum, 1 % antibiotic/antimycotic (100X) solution. Cells were kept in a humidified 95 % air and 5 % CO_2 incubator at 37 °C. TPP stocks were prepared in dimethyl sulfoxide (DMSO). Before cell treatments, TPP dilutions were prepared in medium and DMSO concentrations were adjusted to 0.1 %. Cells were treated with 50 μM, 100 μM and 200 μM TPP concentrations along with control (0.1 % DMSO) for 24 h (h).

2.3. Cell viability assays

The effect of TPP on cell viability was determined using the MTT and Neutral Red Uptake Assays using published procedures (Mosmann, 1983; Repetto et al., 2008). Briefly, the cells were seeded into 96 well plates at a density of 5×10^4 cells/well in 100 μL medium and let to adhere 18–24 h. The next day the cells were treated in a concentration range between 10 and 500 μM TPP concentrations in 100 μL medium for 24 h.

For the MTT assay, the cells were incubated with 0.05 mg/mL MTT for 3 h at 37 °C after TPP treatments. Formed formazan salts were dissolved in DMSO with gentle shaking. The absorbance values were read at 590 nm with an Epoch microplate spectrometer (BioTek).

For the NRU assay, the medium was replaced with 50 μg/mL neutral red in medium and incubated for 3 h at 37 °C. Afterwards, the medium was discarded and the uptaken neutral red by the cells was dissolved with a mixture of acetic acid, water and ethanol (1:49:50). The absorbance was read at 540 nm with an Epoch microplate spectrometer (BioTek). The cell viability was calculated as the percentage of control cells.

Three different concentrations (50, 100, 200 μM) below the IC_{50} values were selected for the subsequent experiments from the cell viability assay results and a careful evaluation of the literature was done to this end (Wang et al., 2020; Wang et al., 2021).

2.4. Colony formation assay

The colony forming capacity of the HaCaT cells was assayed with a previously described method (Crowley et al., 2016). Briefly, a total of 1×10^4 cells were seeded in 6 well plates and were let to adhere 18–24 h. The cells were treated with 50 μM, 100 μM and 200 μM TPP concentrations for 24 h. Then the cells were cultured with fresh medium for one week. Afterwards, cells were fixed with 100% methanol and dyed with 0.5% crystal violet for 10 min (mins). Finally, the wells were rinsed with distilled water and after the plates were air-dried, photographs were captured and the formed colonies were counted.

2.5. Scratch assay

HaCaT cells were seeded in 6 well plates at 2×10^6 cells/well density and were let to adhere 18–24 h. The wound scratch was created as a linear line using a 200 μL sterile pipette tip on the monolayer cells in each well. Then, after the wells were washed with PBS the cells were observed under a microscope and photographs were captured from each well. The locations of the photographs were marked on the wells. After the cells were treated with 50 μM, 100 μM and 200 μM TPP concentrations for 24 h, the cells were observed under a microscope. The photographs were again captured from the marked points of each well. The distance of the cell migration from the wound scratch was calculated in each group via the wound healing tool of Fiji Software.

2.6. Apoptosis necrosis assay

A total of 1×10^6 cells were treated with 50 μM, 100 μM and 200 μM TPP concentrations in 6-well plates for 24 h. After the cells were collected, the apoptosis and necrosis rates were assessed with the Annexin V/Propidium Iodide (PI) dual staining kit according to the manufacturer's protocol (Invitrogen). The cell samples were analyzed using the fluorescence-activated cell sorting (FACS) (BD Bioscience) analysis. The percentages of the apoptotic and necrotic cells were calculated using the Cell Quest program from BD Bioscience.

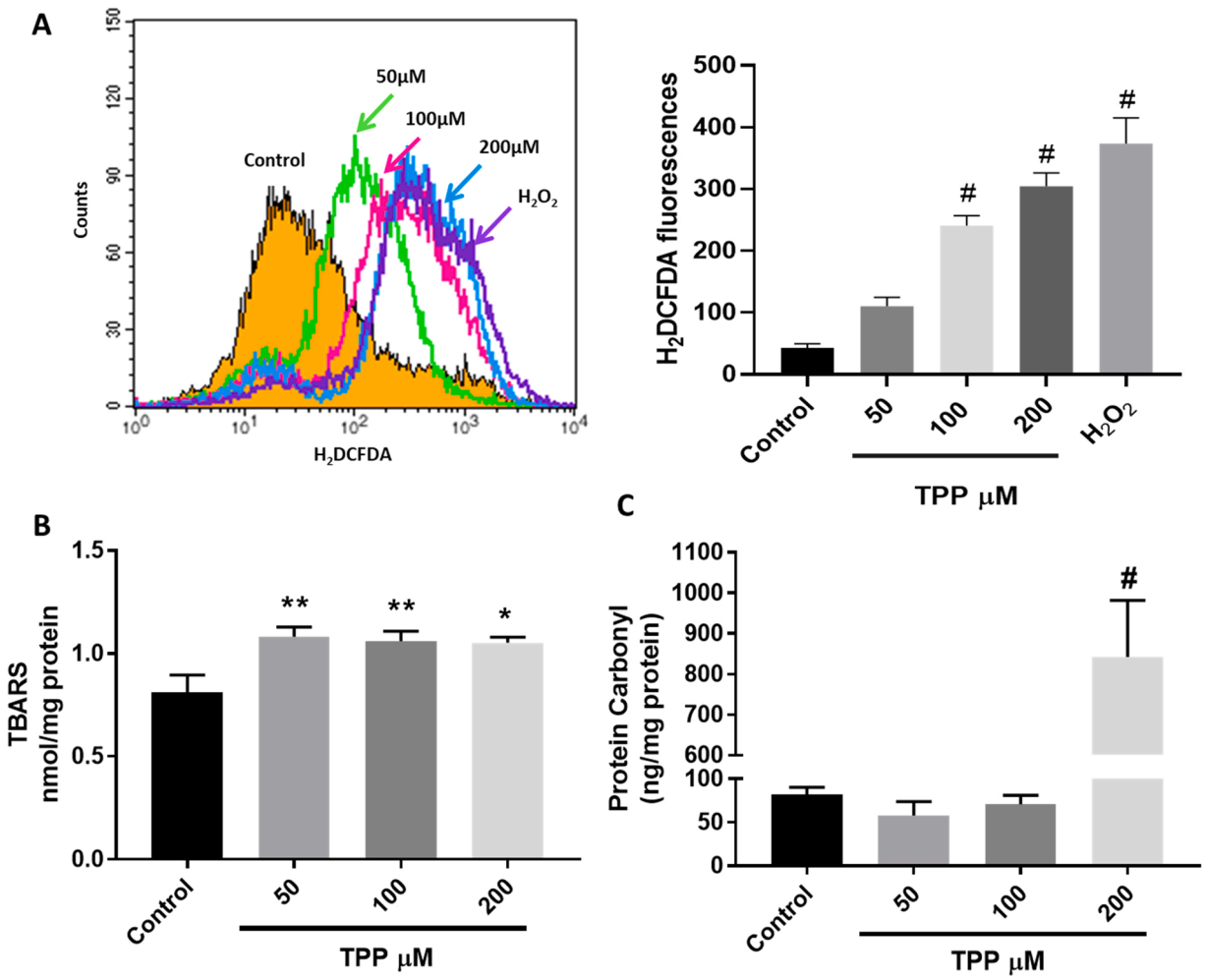

Fig. 4. ROS production (A), lipid peroxidation (B) and protein carbonylation (C) in HaCaT cells after TPP treatment for 24 h. **A.** Representative image and quantitative analysis of flow cytometry-determined ROS production by H_2DCFDA staining. As positive control, HaCaT cells were exposed to 100 μM H_2O_2 for 1 h. **B.** Lipid peroxidation product malondialdehyde level by thiobarbituric acid (TBARS) method. **C.** Protein carbonylation level by human protein carbonyl ELISA assay. Values represent mean ± SD. * $p < 0.05$, * * $p < 0.01$, $^{\#}p < 0.0001$, versus control group.

2.7. Proteasome activity

Similar to the apoptosis necrosis assay, 1×10^6 cells were treated with 50 μM, 100 μM and 200 μM TPP concentrations in 6-well plates for 24 h. The chymotrypsin-like activity of the proteasome was measured with the fluorogenic substrate succinyl-leucine-leucine-valine-tyrosin-methylcoumarine (suc-LLVY-MCA) as previously described (Kisselev and Goldberg, 2005). After TPP exposure, the cell lysates were prepared in buffer containing 250 mM sucrose, 25 mM HEPES, 10 mM $MgCl_2$, 1 mM EDTA and 1 mM DTT by three freeze-thaw cycles and were centrifuged at 15,000 g for 30 mins. 200 μM suc-LLVY-MCA substrate was added to the cell lysates in Tris buffer containing 7.5 mM MgOAc, 7.5 mM $MgCl_2$, 45 mM KCl, and 1 mM DTT. After 30 mins incubation at 37 °C, the fluorescent intensity of liberated MCA was measured at an excitation wavelength of 360 nm and emission wavelength of 460 nm. The protein concentration of the supernatant was measured with the Bradford reagent (Sigma-Aldrich). The MCA liberation was normalized to the protein concentration and time.

2.8. ROS level

Briefly, HaCaT cells were seeded in 96 well plates at 1×10^4 cells/well and were let to adhere for 18–24 h. The next day cells were treated with 50 μM, 100 μM and 200 μM TPP concentrations for 24 h. The cells were treated with 100 μM H_2O_2 for one hour as a positive control. A fluorometric assay with the intracellular oxidation of 5′, 6′-chloromethyl-2′,7′-dichlorofluorescein diacetate (H_2DCFDA) dye was used to determine ROS production as previously described (Eruslanov and Kusmartsev, 2010). After treatments, the cells were incubated with 10 μM H_2DCFDA dye for 30 mins at 37 °C. Following incubation, flow cytometric analysis was carried out with a BD FACS Calibur 4CS flow cytometer. A total of 10000 cells were counted by flow cytometry, the % geometric mean values of the groups were compared. The results were analyzed using the Cell Quest program from BD Bioscience.

2.9. SDS PAGE-western blotting

A total of 5×10^6 cells were treated with 50 μM, 100 μM and 200 μM TPP concentrations for 24 h. After the cells were collected with trypsinization, the cell lysates were prepared in RIPA Buffer and protein concentrations were measured with the Bradford reagent (Sigma-Aldrich). 40 μg proteins were loaded in 10% acrylamide gels and after electrophoresis, the gels were transferred to the nitrocellulose membranes. Then, the membranes were blocked in 5% Tris Buffer Saline with 0.1% Tween-20 (TBST) for 1 h. The membranes were incubated with the following primary antibodies: HSP90, HSP70, GRP94, GRP78 (Cell signaling), polyubiquitin, HSP40 and GAPDH (SCBT), (1:1000). Incubations were made overnight at 4 °C followed by respective secondary

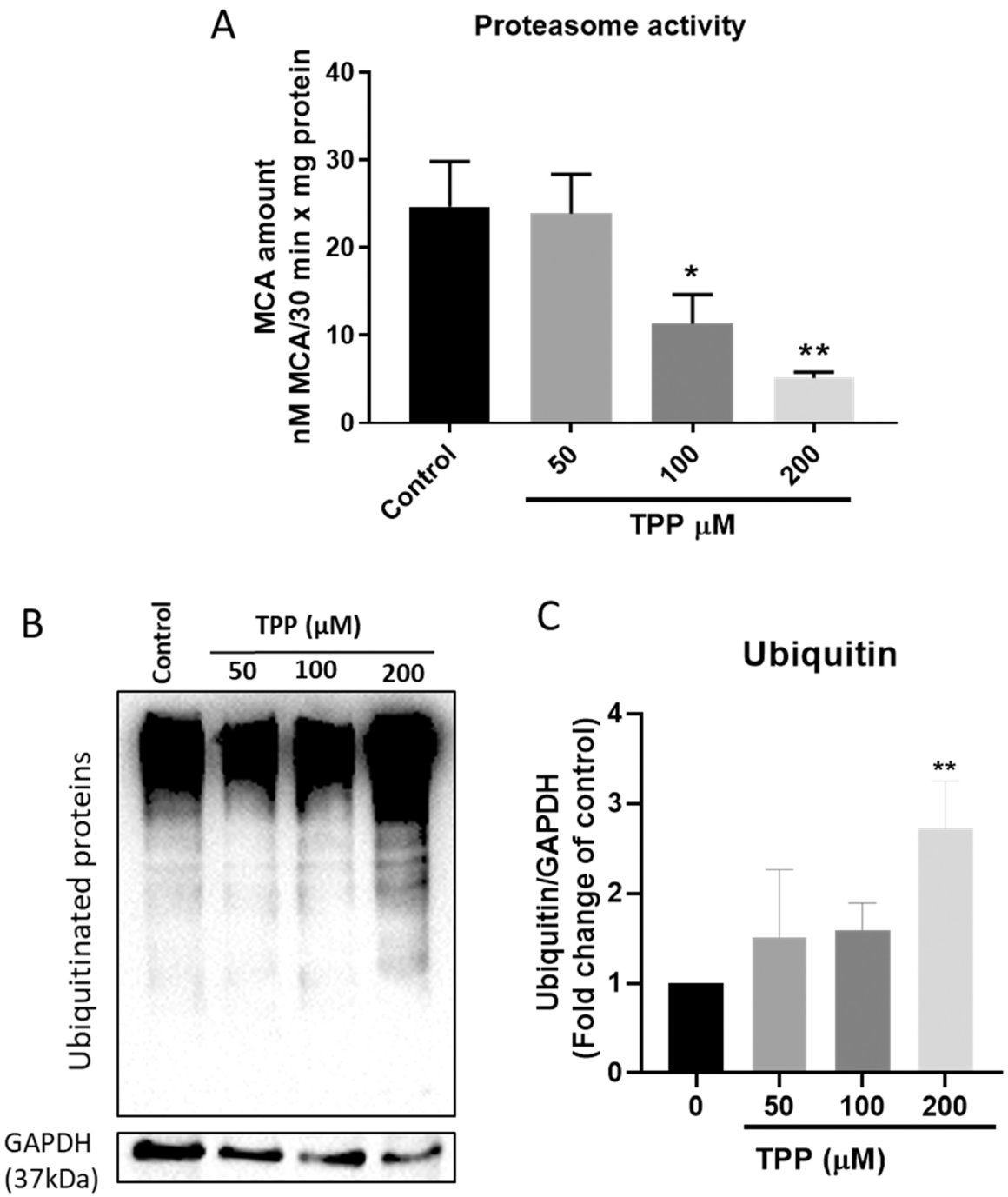

Fig. 5. Proteasome activity (A) and protein ubiquitination (B and C) in HaCaT cells after TPP treatment for 24 h. **A.** Proteasome activity measured by cleavage of fluorogenic substrate suc-LLVY-MCA **B.** Representative images of the protein expression of ubiquitin as detected by western blot. Values represent mean ± SD. * $p < 0.05$, * * $p < 0.01$, versus control group.

antibodies (1:10000) for 2 h at room temperature. The optical densities of protein bands were visualized using an enhanced chemiluminescence detection kit (Invitrogen) by ChemiDoc MP System (Bio-Rad). GAPDH protein was used as the loading control. Image Lab Software (Bio-Rad) was used for quantifying the protein band intensities.

2.10. Malondialdehyde (MDA) level

The level of the lipid peroxidation product malondialdehyde (MDA) was determined with the TBRAS method (Lefevre et al., 1998). Briefly, a total of 1×10^6 cells were treated with 50 μM, 100 μM and 200 μM TPP concentrations for 24 h. After the cells were collected with trypsinization, the cell lysates were prepared and MDA levels were measured with the TBARS Assay Kit according to the manufacturer's protocol (RayBiotek). Protein concentrations of the total cell lysates were measured with the Bradford reagent (Sigma-Aldrich) and the results were expressed as nM MDA/mg protein.

2.11. Protein carbonylation level

For protein carbonylation assay, a total of 1×10^6 cells were treated with 50 μM, 100 μM and 200 μM TPP concentrations for 24 h and collected by trypsinization. Cells were homogenized with three freeze-thaw cycles and brief sonication. Then the cell lysates were obtained

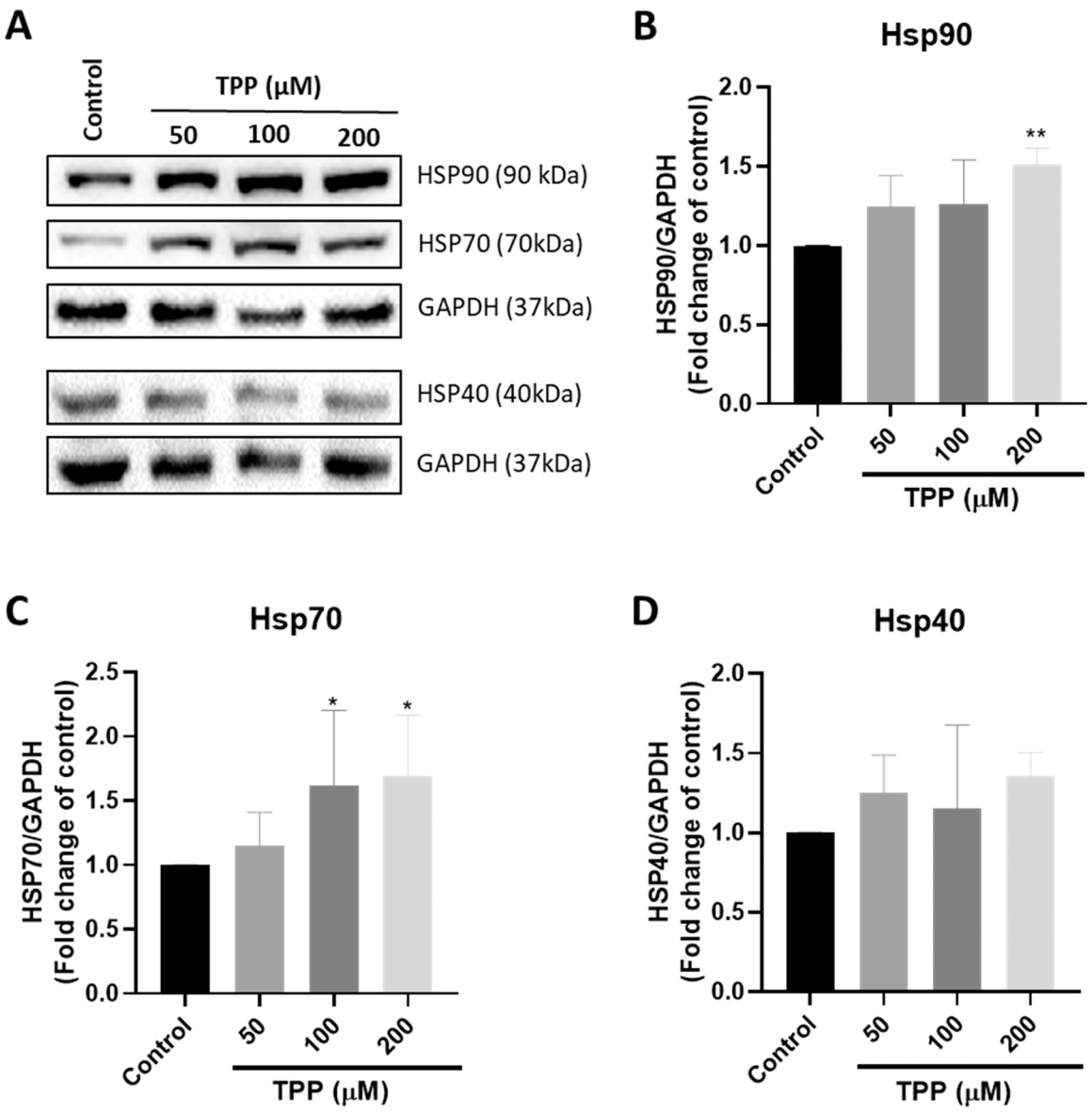

Fig. 6. Western blot results of HSP90 (A and B), HSP70 (A and C) and HSP40 (A and D) proteins in HaCaT cells after TPP treatment for 24 h. **A.** Representative images of the protein expression of HSP90, HSP70 and HSP40, as detected by western blot. **B, C, D.** Quantification of the protein expression of HSP90, HSP70 and HSP40 normalized to those of GAPDH. Values represent mean ± SD. * $p < 0.05$, * * $p < 0.01$, versus control group.

with 13,000 g centrifugation for 15 mins. The protein carbonylation level was measured with the Human Protein Carbonyl Elisa Kit (BT-Lab) following the manufacturer's instructions. The absorbance was measured at 450 nm with a microplate reader (BioTek). Protein concentrations were determined with the Bradford reagent (Sigma-Aldrich) and results were normalized to the protein concentrations.

2.12. Statistical analysis

All experiments were repeated at least three times and the data were expressed as mean ± standard deviation (SD). The IC_{50} values were calculated using the inhibitor-normalized response function in GraphPad Prism 7.0 software. Statistical differences between the treatment groups and control were analyzed by one-way ANOVA followed by Tukey's multiple comparison test as posthoc analysis, again using GraphPad Prism 7.0 software.The level of significance for all statistical analyses was set at P-value < 0.05.

3. Results

3.1. HaCaT cell viability, proliferation and migration were reduced with TPP exposure

According to the MTT and NRU assay results, the cell viability was reduced dose-dependently in HaCaT cells and the IC_{50} values were 214 μM and 257 μM, respectively (Fig. 1).

Further, the effect of TPP on cell migration was evaluated with the colony formation assay. TPP exposure significantly reduced the colony number and no colony formation was observed at 200 μM concentration (Fig. 2A). The cell migration rate was assayed with scratch assay and wound closure % was significantly reduced with 100 μM and 200 μM TPP concentrations (Fig. 2B).

3.2. TPP exposure induced apoptosis in HaCaT cells

Flow cytometry was used with Annexin V/PI staining to determine the effects of TPP on apoptosis of HaCaT cells. The results indicated that

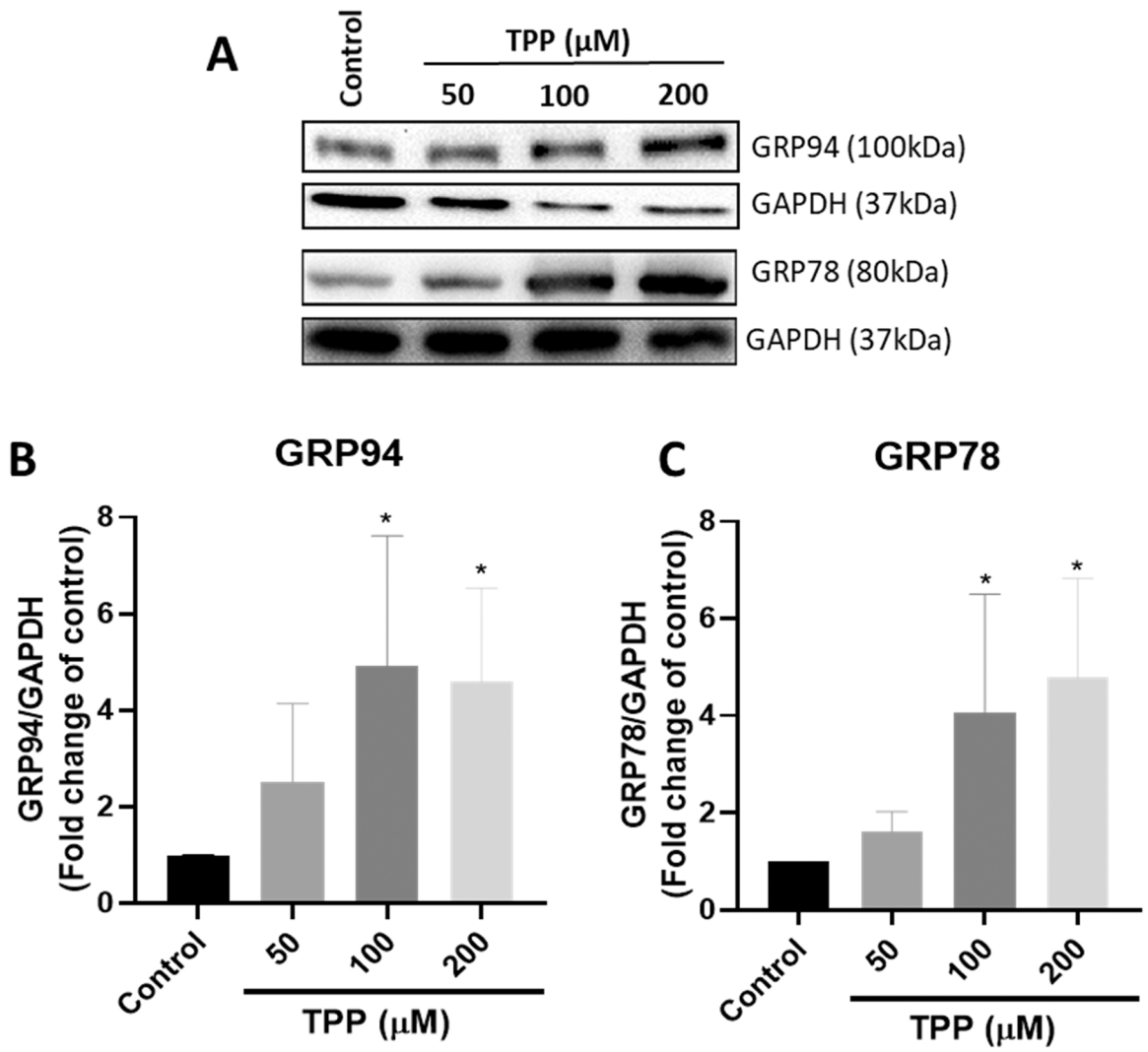

Fig. 7. Western blot results of GRP94 (A and B) and GRP78 (A and C) proteins in HaCaT cells after TPP treatment for 24 h. **A.** Representative images of the protein expression of GRP94 and GRP78, as detected by western blot. **B, C.** Quantification of the protein expression of GRP94 and GRP78 normalized to those of GAPDH. Values represent mean ± SD. * $p < 0.05$, versus control group.

TPP exposure increased the apoptotic cell population significantly in both 100 and 200 μM concentrations compared to control (Fig. 3).

3.3. TPP caused oxidative stress induction, protein carbonylation and lipid peroxidation in HaCaT cells

To investigate whether oxidative stress was involved in TPP toxicity, we examined ROS production using H_2DFCDA staining by flow cytometry. The level of ROS was dose-dependently increased with TPP exposure and this increase was significant at 100 and 200 μM TPP concentrations (Fig. 4A).

To assess the extent of the oxidative stress in HaCaT cells by TPP exposure, MDA and protein carbonylation levels were measured as markers of lipid peroxidation and protein oxidation, respectively. The MDA level significantly increased in all tested concentrations (Fig. 4B) and our results showed that high TPP concentration greatly increased the protein carbonylation level (Fig. 4C).

3.4. TPP exposure decreased proteasome activity and caused the accumulation of ubiquitinated proteins

We examined the proteasome activity and protein ubiquitination level to assess the ubiquitin proteasomal system (UPS) role in TPP toxicity. The proteasome activity was reduced with TPP exposure concentration-dependently and this reduction was significant at 100 and 200 μM concentrations (Fig. 5A). As a result of proteasome inhibition, the ubiquitin-tagged proteins could not be degraded by the proteasomal system and the accumulation of ubiquitinated proteins was increased with TPP exposure in HaCaT cells as can be seen in Fig. 5B, C.

3.5. TPP exposure caused heat shock and endoplasmic reticulum stress in HaCaT cells

The extent of cellular stress after TPP treatment was investigated with HSP90, HSP70, HSP40, GRP94 and GRP78 protein expression analysis. According to the western blot results, TPP exposure increased the protein levels of HSP90 and HSP70, especially at the highest concentration (Fig. 6A-C). However, the protein expression level of HSP40, the cochaperone of HSP70, did not change (Fig. 6A, D).

Next, we aimed to explore ER stress and the protein expression levels of GRP94 and GRP78 were measured. The expression levels of the GRP94 and GRP78 proteins were increased concentration-dependently after TPP exposure in HaCaT cells (Fig. 7A-C) which indicates significant ER stress induction following TPP exposure.

4. Discussion

Since TPP is one of the most commonly used organophosphorus flame retardant additives in many different processes and products, humans are exposed to TPP contaminated environments on a daily basis, which also entails a risk to the environment and human health by releasing significant amounts of TPP into the environment by various routes (van der Veen and de Boer, 2012).

The concentration range of TPP in the aquatic environment and microenvironment is quite wide. For instance, concentrations of TPP range from thousands of ng/g in indoor dust samples to several mg/g in consumer products such as nail polish (Khairy and Lohmann, 2019; Meeker et al., 2013; Mendelsohn et al., 2016; Mizouchi et al., 2015). Also, TPP concentrations have been detected at levels of 96.2 ng/L in seawater and 845 ng/L in wastewater (Kim et al., 2017; Lee et al., 2018; Sun et al., 2022). Due to the widespread use of TPP, human dermal contact with TPP-containing dust is a potentially daily occurrence(Stapleton et al., 2009; Van den Eede et al., 2011). Different study results show that hand wipes, surface wipes, indoor dust and air contain a significant amount of TPP and dermal absorption is an important exposure pathway to TPP (Hoffman et al., 2015; Liu et al., 2018; Xu et al., 2016). As mentioned above, the presence of this agent in nail polish is a significant source of dermal exposure(Tokumura et al., 2019). Although the probability of skin contact with TPP is quite high, there is a lack of studies on the potential adverse effects of TPP on skin health. In the present study, we aimed to study the potential mechanisms of TPP toxicity in a relevant experimental model, that is, the human keratinocyte cell line (HaCaT).

Our results on cytotoxicity with the MTT and NRU assays showed that 24 h of TPP exposure caused cytotoxicity on HaCaT cells. Cytotoxic properties of TPP have been shown with different cell models with similar concentration ranges (An et al., 2016; Van den Eede et al., 2015; Zheng et al., 2018). Based on the IC_{50} values in HaCaT cells and our evaluation of the literature, we chose three different concentrations (50–100–200 μM) for further studies (Wang et al., 2020; X. Wang et al., 2021; Y. Wang et al., 2021).

Since cell migration and proliferation are both necessary components for the proper wound healing of the skin (Ammann et al., 2019), we evaluated the effect of TPP on HaCaT cell proliferation and migration. TPP significantly inhibited the proliferation and cell migration of HaCaT cells in a concentration-dependent manner. Importantly, the decrease in cell viability, the inhibition of cell proliferation and migration, apoptosis, and necrosis were significant with 200 μM concentration of TPP. In broad agreement with our results, Zheng et al. (2018) showed that TPP caused apoptosis induction and inhibition of cell proliferation via cell cycle arrest in HepG2 cells at similar concentrations. The apoptosis/necrosis and cell proliferation assay results support the assertion that cytotoxicity involved the reduction in cell proliferation as well as cell death. ROS form through different reactions due to environmental factors or occur as by-products of normal metabolic processes. The imbalance in the production and scavenging of ROS will result in the oxidative modification of cellular molecules (Stadtman and Levine, 2000). We further examined the effect of TPP on oxidative stress and found elevated ROS production after TPP exposure in HaCaT cells which is consistent with former studies with different models (Chen et al., 2015; Liu et al., 2020; Wang et al., 2020).

Then, we determined whether oxidative stress caused protein and lipid oxidation within the HaCaT cells. According to our results, protein carbonyl levels were greatly increased at the high dose of TPP, which is indicative of protein oxidation. Additionally, MDA level, a by-product of lipid peroxidation, showed a significant increase with all the studied concentrations. Ramesh et al. (2020) also observed increased lipid peroxidation products in the hepatic tissue of a fish model exposed to TPP. Considering other studies showed that TPP can affect the lipid metabolism and lipidome, the lipid peroxidation observed from the low range of concentrations in our study supports that TPP can affect the lipidome (Hu et al., 2020; Van den Eede et al., 2015; Y. Wang et al., 2021). The endoplasmic reticulum (ER) is an organelle that is an important part of the endomembrane system in cells and plays key roles in protein synthesis, posttranslational protein modifications and lipid metabolism (Han and Kaufman, 2016). Disruptions in ER homeostasis result in the activation of a stress response mechanism known as the unfolded protein response (UPR). ER stress-dependent UPR activation plays a critical role in lipid metabolism and homeostasis (Basseri and Austin, 2012). TPP was reported to affect different metabolites related to phospholipid synthesis (Van den Eede et al., 2015), downregulate poly-unsaturation lipids levels (Hu et al., 2020), disturb the lipidome (Y. Wang et al., 2021), and induce ER stress (Hu et al., 2020; Y. Wang et al., 2021). In line with these reports, our results showed that TPP induced ER stress via upregulation of the ER stress proteins, GRP94 and GRP78. Also, important efforts were made to clarify the underlying mechanisms of the effect on adipogenesis and metabolic dysfunction. These studies indicated that TPP is a selective PPARγ modulator (Kim et al., 2020; Y. X. Wang et al., 2021; Y. Wang et al., 2021). A recent study that investigated the TPP effects on adipogenesis on a mouse-derived pre--adipocyte model with a proteomic approach reported that proteasome ubiquitination-related networks were regulated with TPP treatment (Kim et al., 2020). Wang et al. (2020) in a multi-omic study found that TPP caused DNA damage, oncogene activation, redox imbalance and disturbed lipid and protein metabolism to induce hepatotoxicity in human normal liver cells (L02 cells). Also, they reported that the protein expression levels of different proteasome subunits were downregulated with TPP exposure. The proteasome system is the most important protein degradation system in the cells and it degrades more than 80 % of intracellular proteins. Dysregulation of the proteasome increases cellular stress and has been implicated in the pathogenesis of many diseases (Coux et al., 2020).,To the authors' knowledge, no study has focused on the TPP effects on the proteasome activity, therefore, we investigated the impact of TPP on the proteolytic activity of the proteasome. For the first time, we demonstrated that TPP inhibited the proteolytic activity of proteasome and this inhibition was dose-dependent. Indeed, proteasome inhibition leads to the accumulation of ubiquitin-tagged proteasome substrates (Myung et al., 2001). Thus, we further confirmed the proteasome inhibition by determining the level of accumulated ubiquitinated proteins. Our results show that the amount of the ubiquitinated proteins increased in parallel with the dose-dependent decrease in the proteasome activity.

Epidemiologic studies show the presence of organophosphorus flame retardants in both indoor environments and human biological samples. Ubiquitousexposure to agent such as TPP is likely to be linked to various health outcomes related to reproductive, thyroid, respiratory, immune, neuronal and dermal systems (Chupeau et al., 2020; Vuong et al., 2020). Although the keratinocyte model was used in this study, the findings are supported by previous studies which revealed changes in UPS function in other tissues resulting from TPP exposure, such as in adipocyte and liver models (Kim et al., 2020; Wang et al., 2020). What is of concern, is that many neurodegenerative diseases such as Alzheimer's, Huntington's and Parkinson's diseases are associated with disruption of cell homeostasis as a result of aggregates of neurotoxic proteins linked to proteasomal system dysfunction and already TPP has been implicated in neurotoxicity (Hong et al., 2018; Liu et al., 2020). Therefore, it is important to focus on the proteasomal system in future studies examining the effects of TPP on the neuronal system.

Upstream of the proteosome and ER stress-related UPR process, the heat shock chaperone protein system maintains cellular homeostasis through its role in the regulation of protein folding (Kawazoe et al., 1998; Liu and Chang, 2008; Raghunath et al., 2018). Crucially, HSP90 gene expression upregulation has been reported in different toxicity studies of TPP with aquatic organisms: *Daphnia magna* (Yuan et al., 2018), zebrafish embryos (Liu et al., 2013) and *Mytilus galloprovincialis* (Wang et al., 2019). Thus, to further elucidate the extent of the effect of TPP on cellular stress we focused on the protein expression levels of heat

shock proteins. Exposure to TPP caused heat shock response and upregulated the protein expression levels of HSP90 and HSP70. As has been discussed above, TPP inhibits the catalytic activity of the proteasome, increases oxidative stress and consequently affects proteostasis in human keratinocytes.

It should be pointed out that the experimental concentrations employed in this study were much higher than the daily human exposure levels. However, this study evaluated in vitro acute toxic effects and used concentrations that are comparable to many in vitro studies in the literature. Decreases in the levels of genes and proteins related to the ubiquitin proteasomal system have been reported previously with different models and end-points (Hao et al., 2020; Wang et al., 2020; Yuan et al., 2018). Although high concentrations were used in this study, our findings are important in terms of evaluating the effects on populations close to primary pollution sources and providing a better understanding of the molecular toxic effects of TPP.

5. Conclusion

In summary, this is the first report to our knowledge that shows the potential inhibition of proteasome activity in the presence of TPP. The cytotoxic nature of the concentration range in this report is of most relevance to acute exposure of TPP andfurther research with different durations and sub-cytotoxic concentrations may estimate the more subtle impact of this agent in dermal and other human cellular models.

CRediT authorship contribution statement

A.T.J. and B.A. conceptualized the study. A.T.J. and A.M.Y.G designed the experiments. A.T.J. and A.M.Y.G carried out the assays and analyzed the data. A.T.J. wrote the manuscript. All authors participated in the editing and revision of the manuscript.

Declaration of Competing Interest

The authors declare that they have no known competing financial interests or personal relationships that could have appeared to influence the work reported in this paper.

Acknowledgments

We thank Professor Betul Karademir Yilmaz for providing constructive critique on the study. This study was funded in part by the Scientific Research Projects Coordination Unit of Istanbul University. Project number: TAB-2021-37247.

References

Ammann, K.R., DeCook, K.J., Li, M., Slepian, M.J., 2019. Migration versus proliferation as contributor to in vitro wound healing of vascular endothelial and smooth muscle cells. Exp. Cell Res. 376, 58–66. https://doi.org/10.1016/j.yexcr.2019.01.011.

An, J., Hu, J., Shang, Y., Zhong, Y., Zhang, X., Yu, Z., 2016. The cytotoxicity of organophosphate flame retardants on HepG2, A549 and Caco-2 cells. J. Environ. Sci. Health Part A 51, 980–988. https://doi.org/10.1080/10934529.2016.1191819.

Andresen, J.A., Grundmann, A., Bester, K., 2004. Organophosphorus flame retardants and plasticisers in surface waters. Sci. Total Environ. 332, 155–166. https://doi.org/10.1016/j.scitotenv.2004.04.021.

Basseri, S., Austin, R.C., 2012. Endoplasmic reticulum stress and lipid metabolism: mechanisms and therapeutic potential. Biochem. Res. Int. 2012, 1–13. https://doi.org/10.1155/2012/841362.

Betts, K.S., 2015. Tracking alternative flame retardants: hand-to-mouth exposures in adults. Environ. Health Perspect. 123. https://doi.org/10.1289/ehp.123-A44.

Chen, G., Jin, Y., Wu, Y., Liu, L., Fu, Z., 2015. Exposure of male mice to two kinds of organophosphate flame retardants (OPFRs) induced oxidative stress and endocrine disruption. Environ. Toxicol. Pharmacol. 40, 310–318. https://doi.org/10.1016/j.etap.2015.06.021.

Chupeau, Z., Bonvallot, N., Mercier, F., Le Bot, B., Chevrier, C., Glorennec, P., 2020. Organophosphorus flame retardants: a global review of indoor contamination and human exposure in Europe and epidemiological evidence. Int. J. Environ. Res. Public Health 17, 6713.

Coux, O., Zieba, B.A., Meiners, S., 2020. The proteasome system in health and disease. Prote Dis. 55–100.

Crowley, L.C., Christensen, M.E., Waterhouse, N.J., 2016. Measuring survival of adherent cells with the colony-forming assay. Cold Spring Harb. Protoc. 2016 pdb-prot087171.

Eruslanov, E., Kusmartsev, S., 2010. Identification of ROS using oxidized DCFDA and flow-cytometry. In: Advanced Protocols in Oxidative Stress II. Springer, pp. 57–72.

Estill, C.F., Slone, J., Mayer, A., Chen, I.-C., La Guardia, M.J., 2020. Worker exposure to flame retardants in manufacturing, construction and service industries. Environ. Int. 135, 105349 https://doi.org/10.1016/j.envint.2019.105349.

Han, J., Kaufman, R.J., 2016. The role of ER stress in lipid metabolism and lipotoxicity. J. Lipid Res. 57, 1329–1338. https://doi.org/10.1289/ehp.1408669.

Hao, H., Dang, Y., Chen, S., Sun, Q., Kong, R., Cheng, S., Liu, C., 2020. Effects of triphenyl phosphate on ciliate protozoa Tetrahymena thermophila following acute exposure and sub-chronic exposure. Ecotoxicol. Environ. Saf. 200, 110757.

Hoffman, K., Garantziotis, S., Birnbaum, L.S., Stapleton, H.M., 2015. Monitoring Indoor exposure to organophosphate flame retardants: hand wipes and house dust. Environ. Health Perspect. 123, 160–165. https://doi.org/10.1289/ehp.1408669.

Hong, X., Chen, R., Hou, R., Yuan, L., Zha, J., 2018. Triphenyl phosphate (TPHP)-induced neurotoxicity in adult male Chinese rare minnows (Gobiocypris rarus). Environ. Sci. Technol. 52, 11895–11903.

Hu, W., Kang, Q., Zhang, C., Ma, H., Xu, C., Wan, Y., Hu, J., 2020. Triphenyl phosphate modulated saturation of phospholipids: Induction of endoplasmic reticulum stress and inflammation. Environ. Pollut. https://doi.org/10.1016/j.envpol.2020.114474.

Jayatilaka, N.K., Restrepo, P., Davis, Z., Vidal, M., Calafat, A.M., Ospina, M., 2019. Quantification of 16 urinary biomarkers of exposure to flame retardants, plasticizers, and organophosphate insecticides for biomonitoring studies. Chemosphere 235, 481–491. https://doi.org/10.1016/j.chemosphere.2019.06.181.

Jung, T., Catalgol, B., Grune, T., 2009. The proteasomal system. Mol. Asp. Med. https://doi.org/10.1016/j.mam.2009.04.001.

Kawazoe, Y., Nakai, A., Tanabe, M., Nagata, K., 1998. Proteasome inhibition leads to the activation of all members of the heat-shock-factor family. Eur. J. Biochem. 255, 356–362. https://doi.org/10.1046/j.1432-1327.1998.2550356.x.

Khairy, M.A., Lohmann, R., 2019. Organophosphate flame retardants in the indoor and outdoor dust and gas-phase of Alexandria, Egypt. Chemosphere 220, 275–285.

Kim, S., Rabhi, N., Blum, B.C., Hekman, R., Wynne, K., Emili, A., Farmer, S., Schlezinger, J.J., 2020. Triphenyl phosphate is a selective PPARγ modulator that does not induce brite adipogenesis in vitro and in vivo. Arch. Toxicol. 94, 3087–3103. https://doi.org/10.1007/s00204-020-02815-1.

Kim, U.-J., Oh, J.K., Kannan, K., 2017. Occurrence, removal, and environmental emission of organophosphate flame retardants/plasticizers in a wastewater treatment plant in New York State. Environ. Sci. Technol. 51, 7872–7880.

Kisselev, A.F., Goldberg, A.L., 2005. Monitoring activity and inhibition of 26S proteasomes with fluorogenic peptide substrates. Methods Enzym. 398, 364–378.

Kojima, H., Takeuchi, S., Itoh, T., Iida, M., Kobayashi, S., Yoshida, T., 2013. In vitro endocrine disruption potential of organophosphate flame retardants via human nuclear receptors. Toxicology 314, 76–83. https://doi.org/10.1016/j.tox.2013.09.004.

Lee, S., Cho, H.-J., Choi, W., Moon, H.-B., 2018. Organophosphate flame retardants (OPFRs) in water and sediment: Occurrence, distribution, and hotspots of contamination of Lake Shihwa, Korea. Mar. Pollut. Bull. 130, 105–112.

Lefevre, G., Beljean-Leymarie, M., Beyerle, F., Bonnefont-Rousselot, D., Cristol, J.-P., Therond, P., Torreilles, J., 1998. Evaluation of lipid peroxidation by assaying the thiobarbituric acid-reactive substances. Ann. De. Biol. Clin. 305–319.

Li, J., Yu, N., Zhang, B., Jin, L., Li, M., Hu, M., Zhang, X., Wei, S., Yu, H., 2014. Occurrence of organophosphate flame retardants in drinking water from China. Water Res. 54, 53–61. https://doi.org/10.1016/j.watres.2014.01.031.

Liu, C., Wang, Q., Liang, K., Liu, J., Zhou, B., Zhang, X., Liu, H., Giesy, J.P., Yu, H., 2013. Effects of tris(1,3-dichloro-2-propyl) phosphate and triphenyl phosphate on receptor-associated mRNA expression in zebrafish embryos/larvae. Aquat. Toxicol. 128–129, 147–157. https://doi.org/10.1016/j.aquatox.2012.12.010.

Liu, X., Ji, K., Choi, K., 2012. Endocrine disruption potentials of organophosphate flame retardants and related mechanisms in H295R and MVLN cell lines and in zebrafish. Aquat. Toxicol. 114–115, 173–181. https://doi.org/10.1016/j.aquatox.2012.02.019.

Liu, X., Yu, G., Cao, Z., Wang, B., Huang, J., Deng, S., Wang, Y., 2017. Occurrence of organophosphorus flame retardants on skin wipes: insight into human exposure from dermal absorption. Environ. Int. 98, 113–119. https://doi.org/10.1016/j.envint.2016.10.021.

Liu, X., Cao, Z., Yu, G., Wu, M., Li, X., Zhang, Y., Wang, B., Huang, J., 2018. Estimation of exposure to organic flame retardants via hand wipe, surface wipe, and dust: comparability of different assessment strategies. Environ. Sci. Technol. 52, 9946–9953. https://doi.org/10.1021/acs.est.8b02723.

Liu, X., Zhao, X., Wang, Y., Hong, J., Shi, M., Pfaff, D., Guo, L., Tang, H., 2020. Triphenyl phosphate permeates the blood brain barrier and induces neurotoxicity in mouse brain. Chemosphere 252, 126470. https://doi.org/10.1016/j.chemosphere.2020.126470.

Liu, Y., Chang, A., 2008. Heat shock response relieves ER stress. EMBO J. 27, 1049–1059. https://doi.org/10.1038/emboj.2008.42.

Meeker, J.D., Stapleton, H.M., 2010. House dust concentrations of organophosphate flame retardants in relation to hormone levels and semen quality parameters. Environ. Health Perspect. 118, 318–323. https://doi.org/10.1289/ehp.0901332.

Meeker, J.D., Cooper, E.M., Stapleton, H.M., Hauser, R., 2013. Urinary metabolites of organophosphate flame retardants: temporal variability and correlations with house dust concentrations. Environ. Health Perspect. 121, 580–585.

Mendelsohn, E., Hagopian, A., Hoffman, K., Butt, C.M., Lorenzo, A., Congleton, J., Webster, T.F., Stapleton, H.M., 2016. Nail polish as a source of exposure to triphenyl phosphate. Environ. Int. 86, 45–51. https://doi.org/10.1016/j.envint.2015.10.005.

Mizouchi, S., Ichiba, M., Takigami, H., Kajiwara, N., Takamuku, T., Miyajima, T., Kodama, H., Someya, T., Ueno, D., 2015. Exposure assessment of organophosphorus and organobromine flame retardants via indoor dust from elementary schools and domestic houses. Chemosphere 123, 17–25.

Mosmann, T., 1983. Rapid colorimetric assay for cellular growth and survival: application to proliferation and cytotoxicity assays. J. Immunol. Methods 65, 55–63.

Myung, J., Kim, K.B., Crews, C.M., 2001. The ubiquitin-proteasome pathway and proteasome inhibitors. Med. Res. Rev. 21, 245–273. https://doi.org/10.1002/med.1009.

Qi, Z., Chen, M., Song, Y., Wang, X., Li, B., Chen, Z., Tsang, S.Y., Cai, Z., 2019. Acute exposure to triphenyl phosphate inhibits the proliferation and cardiac differentiation of mouse embryonic stem cells and zebrafish embryos. J. Cell. Physiol. 234, 21235–21248. https://doi.org/10.1002/jcp.28729.

Raghunath, A., Panneerselvam, L., Sundarraj, K., Perumal, E., 2018. Heat shock proteins and endoplasmic reticulum stress. In: Heat Shock Proteins and Stress. Springer, pp. 39–78.

Ramesh, M., Angitha, S., Haritha, S., Poopal, R.-K., Ren, Z., Umamaheswari, S., 2020. Organophosphorus flame retardant induced hepatotoxicity and brain AChE inhibition on zebrafish (Danio rerio. Neurotoxicol. Teratol. 82, 106919 https://doi.org/10.1016/j.ntt.2020.106919.

Repetto, G., Del Peso, A., Zurita, J.L., 2008. Neutral red uptake assay for the estimation of cell viability/cytotoxicity. Nat. Protoc. 3, 1125.

Saito, I., Onuki, A., Seto, H., 2007. Indoor organophosphate and polybrominated flame retardants in Tokyo. Indoor Air 17, 28–36. https://doi.org/10.1111/j.1600-0668.2006.00442.x.

Stadtman, E.R., Levine, R.L., 2000. Protein oxidation. Ann. N. Y. Acad. Sci. 899, 191–208.

Stapleton, H.M., Klosterhaus, S., Eagle, S., Fuh, J., Meeker, J.D., Blum, A., Webster, T.F., 2009. Detection of organophosphate flame retardants in furniture foam and U.S. house dust. Environ. Sci. Technol. 43, 7490–7495. https://doi.org/10.1021/es9014019.

Sun, Z., Ma, W., Tang, X., Zhang, Xin, Yang, Y., Zhang, Xinxin, 2022. Toxicity of triphenyl phosphate toward the marine rotifer Brachionus plicatilis: changes in key life-history traits, rotifer-algae population dynamics and the metabolomic response. Ecotoxicol. Environ. Saf. 241, 113731.

Tokumura, M., Seo, M., Wang, Q., Miyake, Y., Amagai, T., Makino, M., 2019. Dermal exposure to plasticizers in nail polishes: an alternative major exposure pathway of phosphorus-based compounds. Chemosphere 226, 316–320. https://doi.org/10.1016/j.chemosphere.2019.03.108.

Van den Eede, N., Dirtu, A.C., Neels, H., Covaci, A., 2011. Analytical developments and preliminary assessment of human exposure to organophosphate flame retardants from indoor dust. Environ. Int. 37, 454–461. https://doi.org/10.1016/j.envint.2010.11.010.

Van den Eede, N., Cuykx, M., Rodrigues, R.M., Laukens, K., Neels, H., Covaci, A., Vanhaecke, T., 2015. Metabolomics analysis of the toxicity pathways of triphenyl phosphate in HepaRG cells and comparison to oxidative stress mechanisms caused by acetaminophen. Toxicol. Vitr. 29, 2045–2054. https://doi.org/10.1016/j.tiv.2015.08.012.

van der Veen, I., de Boer, J., 2012. Phosphorus flame retardants: properties, production, environmental occurrence, toxicity and analysis. Chemosphere 88, 1119–1153. https://doi.org/10.1016/j.chemosphere.2012.03.067.

Vuong, A.M., Yolton, K., Cecil, K.M., Braun, J.M., Lanphear, B.P., Chen, A., 2020. Flame retardants and neurodevelopment: an updated review of epidemiological literature. Curr. Epidemiol. Rep. 7, 220–236.

Wang, D., Zhu, W., Chen, L., Yan, J., Teng, M., Zhou, Z., 2018. Neonatal triphenyl phosphate and its metabolite diphenyl phosphate exposure induce sex- and dose-dependent metabolic disruptions in adult mice. Environ. Pollut. 237, 10–17. https://doi.org/10.1016/j.envpol.2018.01.047.

Wang, D., Yan, S., Yan, J., Teng, M., Meng, Z., Li, R., Zhou, Z., Zhu, W., 2019. Effects of triphenyl phosphate exposure during fetal development on obesity and metabolic dysfunctions in adult mice: impaired lipid metabolism and intestinal dysbiosis. Environ. Pollut. https://doi.org/10.1016/j.envpol.2018.12.053.

Wang, X., Li, F., Liu, J., Ji, C., Wu, H., 2020. Transcriptomic, proteomic and metabolomic profiling unravel the mechanisms of hepatotoxicity pathway induced by triphenyl phosphate (TPP. Ecotoxicol. Environ. Saf. 205, 111126 https://doi.org/10.1016/j.ecoenv.2020.111126.

Wang, X., Li, F., Liu, J., Li, Q., Ji, C., Wu, H., 2021. New insights into the mechanism of hepatocyte apoptosis induced by typical organophosphate ester: an integrated in vitro and in silico approach. Ecotoxicol. Environ. Saf. 219, 112342 https://doi.org/10.1016/j.ecoenv.2021.112342.

Wang, Y., Hong, J., Shi, M., Guo, L., Liu, L., Tang, H., Liu, X., 2021. Triphenyl phosphate disturbs the lipidome and induces endoplasmic reticulum stress and apoptosis in JEG-3 cells. Chemosphere 275, 129978. https://doi.org/10.1016/j.chemosphere.2021.129978.

WHO, World Health Organization, 1991. Triphenyl phosphate/published under the joint sponsorship of the United Nations Environment Programme, the International Labour Organisation, and the World Health Organization. In: Triphenyl Phosphate/Published under the Joint Sponsorship of the United Nations Environment Programme, the International Labour Organisation, and the. World Health Organization.

Xu, F., Giovanoulis, G., Van Waes, S., Padilla-Sanchez, J.A., Papadopoulou, E., Magnér, J., Haug, L.S., Neels, H., Covaci, A., 2016. Comprehensive study of human external exposure to organophosphate flame retardants via air, dust, and hand wipes: the importance of sampling and assessment strategy. Environ. Sci. Technol. 50, 7752–7760.

Yuan, S., Li, H., Dang, Y., Liu, C., 2018. Effects of triphenyl phosphate on growth, reproduction and transcription of genes of Daphnia magna. Aquat. Toxicol. 195, 58–66. https://doi.org/10.1016/j.aquatox.2017.12.009.

Zhang, Y., Zheng, X., Wei, L., Sun, R., Guo, H., Liu, X., Liu, S., Li, Y., Mai, B., 2018. The distribution and accumulation of phosphate flame retardants (PFRs) in water environment. Sci. Total Environ. 630, 164–170. https://doi.org/10.1016/j.scitotenv.2018.02.215.

Zheng, K., Zhong, Y., Yu, Z., Shang, Y., An, J., 2018. Triphenyl phosphate (TPP) and tris (2-chloroisopropyl) phosphate (TCPP) induced apoptosis and cell cycle arrest in HepG2. Cells. https://doi.org/10.25177/JESES.4.1.RA.409.